Sharif University of Technology

Scientia Iranica

Transactions on Mechanical Engineering

https://scientiairanica.sharif.edu

Numerical simulation of laminar flow and free convection heat transfer from an isothermal vertical flat plate

Ali Belhocine [a,*], Nadica Stojanovic [b], Oday Ibraheem Abdullah [c]

a. Department of Mechanical Engineering, University of Sciences and the Technology of Oran, L.P 1505 El-MNAOUER, USTO 31000 Oran, Algeria.
b. Department of Motor Vehicles and Motors, Faculty of Engineering, University of Kragujevac, 6 SestreJanjić STR., 34000 Kragujevac, Serbia.
c. Department of System Technologies and Mechanical Design Methodology, Hamburg University of Technology, Hamburg, Germany.

* Corresponding author: al.belhocine@yahoo.fr (A. Belhocine)

Received 10 September 2022; received in revised form 13 January 2023; accepted 30 August 2023

Keywords

Natural convective;
Laminar flow;
Boussinesq approximation;
Vertical plate;
Similarity transformation;
Boundary layer;
Runge-Kutta (RK04) technique.

Abstract

In this modest work, we present a numerical study of the phenomenon of laminar natural convection in a vertical plate, whose wall was maintained at a constant temperature. It was assumed that the boundary layer problem was initially given in a two-dimensional flow even though the physical properties of the fluid were considered to be constant except for the density change with the temperature. The governing equations of the model have been transformed and simplified into a non-linear system of Ordinary Differential Equations (ODE) through the use of similarity variables which we were able to solve numerically using the Runge-Kutta method. This method has better opted for the numerical resolution of this system which was developed in FORTRAN code on the computer. The numerical results of the model were presented in tabular form and the velocity and temperature profiles for various Prandtl numbers were analyzed and depicted graphically. Also, the expressions of the mean heat transfer rate and the average Nusselt number for the whole plate were obtained in the analysis. The results were compared at the end with the numerical results obtained in the literature, showing that they were in good agreement.

1. Introduction

The numerical simulation of heat transfer by natural convection in vertical pipes has aroused growing interest in recent decades. In everyday life and the field of industry, the phenomenon of natural convection is used in several industrial applications [1]. Bhuvaneswari et al. [2] resorted to the use of the similarity variable in order to study on a convective flow the effects of viscous dissipation. Sepahi-Younsi et al. [3] investigated experimentally boundary layer problem for free flow. Saeidinezhad et al. [4] analyzed both, pressure distributions on the surface and the boundary layer. Golkar et al. [5] have experimentally studied on a horizontal flat plate, a heat transfer from a nanofluid. In the work done by Shakiba and Rahimi [6], the Boussinesq approximation was used to numerically analyze an unsteady flow problem in mixed convection. Lakshmi Devi et al. [7] used similarity transformations to analyze nanofluid flow while visualizing the effects of buoyancy force. A numerical analysis was conducted by Mokaddes Ali et al. [8] in order to study a mixed convective flow. Other numerical investigations were carried out in this field on fluid flows [9,10].

Alomar et al. [11] numerically studied a natural convection problem in a bank carrying orthogonal and heating plates. Through a cylindrical tube, a fluid in viscous flow subjected to free convection has been examined by Shah et al. [12].

To cite this article:
A. Belhocine, N. Stojanovic, O.I. Abdullah "Numerical simulation of laminar flow and free convection heat transfer from an isothermal vertical flat plate", *Scientia Iranica* (2025); **32**(6): 7139. https://doi.org/10.24200/sci.2023.61098.7139

Awan et al. [13] performed a numerical simulation on the free convective heat transfer of two vertical plates. Awan et al. [14] made a simulation of a ferrofluid subjected to a flow in free convection. Qasim et al. [15] examined in a vertical circular tube, an incompressible flowing fluid with a free convection mechanism. Awan et al. [16] performed a study on convective flow through a vertical plate. Kim et al. [17] analyzed air in natural convection penetrating vertical and parallel plates.

Another numerical study on natural convection was expressed by Kandaswamy et al. [18]. Ismaeel et al. [19] mathematically simulated a heat transport model using similarity variables. Hady et al. [20] numerically analyzed the natural convection in a vertical plate.

The case of a natural convection flow generated by the presence of a boundary layer in a vertical plate configuration has been observed experimentally by Talluru et al. [21].

In the works given by Belhocine et al. [22-26], it has been interesting to involve the resolution of the heat equation by certain iterative numerical methods and other analytical procedures. A numerical study of natural convection in a vertical plate under laminar flow using the similarity approach has been reported by Jena and Mathur [27]. The main goal of our study is to develop a purely numerical analysis in order to solve a two-dimensional boundary layer problem in laminar natural convection within a vertical flat plate which has several practical applications.

The motivation of the research and the novelty here is to resort to the procedure of similarity of the variables associated with the Runge-Kutta method, which constitutes the most efficient solution to solve such a problem. The advantage of the RK04 method involved here is to give results in better acuity with more precise numerical values. The Navier Stokes equations that describe the motion of fluids were first simplified using asymptotic boundary layer theories, and then they were reduced to a group of equations including the iterative Runge-Kutta method, written in FORTRAN is widely known for its resolution.

Under the angle of the numerical simulation, we obtained the essential results of fields of velocity, and temperatures, in terms of the number of Prandtl where they were schematized on figures and discussed carefully of which particular attention was given to the rate of heat transfer to the wall. In order to check the accuracy of the numerical results, the present results were compared with the available results of Jena and Mathur [27], Ostrach [28] and were found to be in excellent agreement which automatically leads to the validation of the results of our numerical simulation.

2. General formulation of natural convection equations

2.1. Natural convection on an inclined surface

The governing equations of fluid dynamics-namely; the continuity, momentum, and energy equations aredefined as follows:

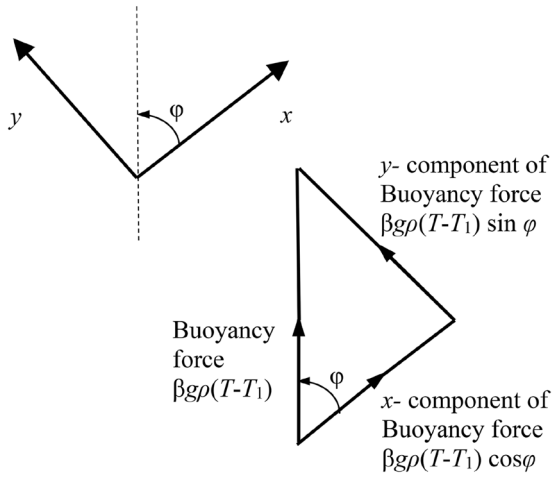

Figure 1. Diagram defining the buoyancy force components.

$$\frac{D\rho}{Dt} + \rho\,\nabla.\vec{V} = 0, \tag{1}$$

$$\rho\,\frac{D\vec{V}}{Dt} = \rho\,\vec{g} - \nabla\vec{p} + \frac{1}{3}\mu\nabla\left(\nabla.\vec{V}\right) + \mu\nabla^2\vec{V}, \tag{2}$$

$$\rho c_P \frac{DT}{Dt} = \nabla.k\nabla T + \beta T\frac{Dp}{Dt} + \mu\Phi + q'''. \tag{3}$$

With Φ is called the dissipation function, defined by:

$$\Phi = \left[\begin{array}{c} 2\left(\frac{\partial u}{\partial x}\right)^2 + 2\left(\frac{\partial v}{\partial y}\right)^2 + 2\left(\frac{\partial w}{\partial z}\right)^2 + \left(\frac{\partial u}{\partial y} + \frac{\partial v}{\partial x}\right)^2 \\ + \left(\frac{\partial v}{\partial z} + \frac{\partial w}{\partial y}\right)^2 + \left(\frac{\partial w}{\partial x} + \frac{\partial u}{\partial z}\right)^2 - \frac{2}{3}\left(\frac{\partial u}{\partial x} + \frac{\partial v}{\partial y} + \frac{\partial w}{\partial z}\right)^2 \end{array}\right]$$

By replacing p with the piezometric pressure, defined by the expression $p' = p + \rho_0 g$, Eq. (2) will take the following form:

$$\frac{D\vec{V}}{Dt} = (\rho - \rho_0)\,\vec{g} - \nabla\overrightarrow{p'} + \frac{1}{3}\mu\nabla\left(\nabla.\vec{V}\right) + \mu\nabla^2\vec{V}. \tag{4}$$

The schematic of the buoyancy force components used in the analysis is shown in Figure 1.

In order to facilitate the solution of the thermal problem, we took into account the following assumptions: the physical properties of the fluid are constant, the flow is considered incompressible, and at steady state in two dimensions, the dissipation Φ, and the heat source q'' are negligible.

According to the Boussinesq approximation, the buoyancy force can be given as:

$(\rho_0 - \rho) = g\,\rho_0\,\beta(T - T_1)$.

After applying the above, we obtain the following system of equations [29]:

$$\frac{\partial u}{\partial x} + \frac{\partial v}{\partial y} = 0, \tag{5}$$

$$u\frac{\partial u}{\partial x} + v\frac{\partial u}{\partial y} = -\frac{1}{\rho}\frac{\partial p}{\partial x} + \nu\left(\frac{\partial^2 u}{\partial x^2} + \frac{\partial^2 u}{\partial y^2}\right) + \beta g(T - T_1)\cos\varphi, \tag{6}$$

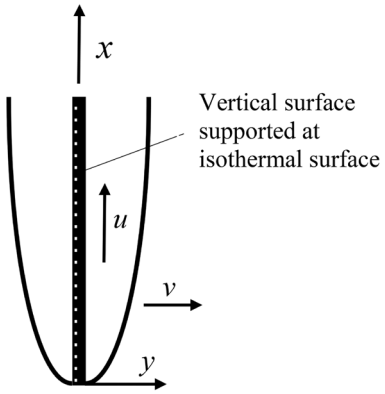

Figure 2. Schematic representation of the model.

$$u\frac{\partial v}{\partial x}+v\frac{\partial v}{\partial y}=-\frac{1}{\rho}\frac{\partial p}{\partial x}+\nu\left(\frac{\partial^2 v}{\partial x^2}+\frac{\partial^2 v}{\partial y^2}\right)+\beta g(T-T_1)\sin\varphi, \quad (7)$$

$$u\frac{\partial T}{\partial x}+v\frac{\partial T}{\partial y}=\left(\frac{k}{\rho c_p}\right)\left(\frac{\partial^2 T}{\partial x^2}+\frac{\partial^2 T}{\partial y^2}\right). \quad (8)$$

where T_1 is the temperature in the undisturbed fluid far from the surface and the pressure, and φ is the angle between the verticaland x-axis.

3. Mathematical formulation of the problem

3.1. Physical configuration

The model we have treated is well illustrated in Figure 2.

According to the assumptions of the boundary layer, our thermal problem consists in simultaneously solving the following system of equations:

$$\frac{\partial u}{\partial x}+\frac{\partial v}{\partial y}=0, \quad (9)$$

$$u\frac{\partial u}{\partial x}+v\frac{\partial u}{\partial y}=\left(\frac{\mu}{\rho}\right)\frac{\partial^2 u}{\partial y^2}+\beta g(T-T_1), \quad (10)$$

$$u\frac{\partial T}{\partial x}+v\frac{\partial T}{\partial y}=\left(\frac{k}{\rho c_p}\right)\frac{\partial^2 T}{\partial y^2}. \quad (11)$$

With the following boundary conditions:

$$\text{At}\quad y=0:\ u=v=0\ ,\ T=T_w,$$
$$\text{For large}\quad y\ :\ u\to 0\ ,\ T\to T_1. \quad (12)$$

3.2. Numerical model based on the similarity solution

If we suppose for all the values of x that the temperature and the velocity are kept similar:

$$\frac{u}{u_r}=\text{function}\left(\frac{y}{\delta}\right),$$

and

$$\frac{T-T_1}{T_w-T_1}=\text{function}\left(\frac{y}{\delta}\right).$$

With δ and u_r denoting respectively the thickness of the boundary layer and the reference velocity

The Grashof number, Gr_x by definition is expressed as a function of x, like this:

$$Gr_x=\frac{\beta g(T_w-T_1)x^3}{\upsilon^2}.$$

The variable η can be considered as a function only of y/δ, so:

$$\eta=\frac{y}{x}Gr_x^{0.25}. \quad (13)$$

For the flow, the velocity is simply written:

$$u_r=\sqrt{\beta g(T_w-T_1)x}.$$

The expression of the velocity and the temperature are then written like this:

$$\frac{u}{\sqrt{\beta g(T_w-T_1)x}}=F'(\eta), \quad (14)$$

and

$$\frac{T-T_1}{T_w-T_1}=G(\eta). \quad (15)$$

In order to make the previous dimensionless equations, they will be transformed by the following relations:

$$U=\frac{u}{\sqrt{\beta g(T_w-T_1)x}}=\left(\frac{ux}{\upsilon}\right)Gr_x^{-0.5},$$
$$V=\frac{v}{\sqrt{\beta g(T_w-T_1)x}}=\left(\frac{vx}{\upsilon}\right)Gr_x^{-0.5},$$
$$\theta=\frac{(T-T_1)}{(T_w-T_1)}. \quad (16)$$

Substituting into Eq. (9), we get:

$$\frac{\partial}{\partial x}\left[U\sqrt{\beta g(T_w-T_1)x}\right]+\frac{\partial}{\partial y}\left[V\sqrt{\beta g(T_w-T_1)x}\right]=0.$$

Which give:

$$\frac{\partial U}{\partial x}+\frac{U}{2x}+\frac{\partial V}{\partial y}=0. \quad (17)$$

By involving the similarity variable, η, this equation will transform into:

$$\frac{\partial U}{\partial \eta}\frac{\partial \eta}{\partial x}+\frac{U}{2x}+\frac{\partial V}{\partial \eta}\frac{\partial \eta}{\partial y}=0. \quad (18)$$

The partial derivatives of η with respect to x and y yield us:

$$\frac{\partial \eta}{\partial x}=-\frac{y}{4x^2}Gr_x^{0.25}=-\frac{\eta}{4x}, \quad (19)$$

$$\frac{\partial \eta}{\partial y}=\frac{Gr_x^{0.25}}{x}. \quad (20)$$

Eq. (18) will take the following form, after replacing these terms:

$$\frac{dF'}{d\eta}\left(-\frac{\eta}{4x}\right)+\frac{F'}{2x}+\frac{\partial V}{\partial \eta}\frac{Gr_x^{0.25}}{x}=0.$$

After calculation and simplification, we get:

$$\frac{\partial V}{\partial \eta}=\frac{1}{2Gr_x^{0.25}}\left[\frac{\eta}{2}\frac{dF'}{d\eta}-F'\right]. \quad (21)$$

The boundary condition in dimensionless form can be written as:

$$\text{At} \quad \eta=0 \ : \ V=0.$$

Integrating Eq. (21) and applying the boundary conditions gives us:

$$V=\frac{1}{2Gr_x^{0.25}}\left[\int \frac{\eta}{2}\frac{dF'}{d\eta}d\eta-F\right],$$

which tend towards:

$$V=\frac{1}{2Gr_x^{0.25}}\left[\frac{\eta F'}{2}-\frac{F}{2}-F\right],$$

from where:

$$V=\frac{1}{4Gr_x^{0.25}}[\eta F'-3F]. \quad (22)$$

By integrating by parts, the first localized term between the square brackets, we will have the relation:

$$\int \frac{\eta}{2}\frac{dF'}{d\eta}d\eta=\int \frac{d}{d\eta}\left(\frac{\eta}{2}F'\right)d\eta-\int \frac{F'}{2}d\eta.$$

The momentum equation will become after the implication of the dimensionless variables:

$$U\frac{\partial U}{\partial x}+\frac{U^2}{2x}+V\frac{\partial U}{\partial y}=v\frac{\partial^2 U}{\partial y^2}\frac{1}{\sqrt{\beta g(T_w-T_1)x}}+\frac{\theta}{x},$$

or in another form:

$$U\frac{\partial U}{\partial \eta}\frac{\partial \eta}{\partial x}+\frac{U^2}{2x}+V\frac{\partial U}{\partial \eta}\frac{\partial \eta}{\partial y}=v\frac{\partial^2 U}{\partial \eta^2}\left(\frac{\partial \eta}{\partial y}\right)\frac{1}{\sqrt{\beta g(T_w-T_1)x}}+\frac{\theta}{x},$$

Whence:

$$F'F''\left(-\frac{\eta}{4x}\right)+\frac{F'^2}{2x}+\frac{1}{4Gr_x^{0.25}}(\eta F'-3F)F''\frac{Gr_x^{0.25}}{x}=\frac{F'''}{x}+\frac{\theta}{x}.$$

From where:

$$-\frac{\eta F'F''}{4}+\frac{F'^2}{2}+\frac{\eta F'F''}{4}-\frac{3FF''}{4}=F'''+G.$$

Finally, we get:.

$$F'''+\frac{3FF''}{4}-\frac{F'^2}{2}+G=0. \quad (23)$$

The energy equation can be expressed as follows:

$$U\frac{\partial \theta}{\partial x}+V\frac{\partial \theta}{\partial y}=\left(\frac{k}{\rho c_p}\right)\frac{\partial^2 \theta}{\partial y^2}\frac{1}{\sqrt{\beta g(T_w-T_1)x}}.$$

So we pull:

$$F'G'\left(-\frac{\eta}{4x}\right)+\frac{1}{4Gr_x^{0.25}}(\eta F'-3F)G'\frac{Gr_x^{0.25}}{x}=\frac{G''}{Pr\,x}.$$

We therefore obtain:

$$G''+\frac{3}{4}Pr\,F\,G'=0. \quad (24)$$

Eqs. (23) and (24) constitute a system of simultaneous Ordinary Differential Equations (ODEs) for the velocity F and temperature functions G.

Then the boundary conditions in the dimensional form are summarized as this:

$$\begin{aligned}&\text{At} \quad y=0: u=0 \ \Rightarrow \ \eta=0: F'=0.\\ &\text{At} \quad y=0: v=0 \ \Rightarrow \ \eta=0: F=0.\\ &\text{At} \quad y=0: T=T_w \ \Rightarrow \ \eta=0: G=1.\\ &\text{For large} \quad y: u\to 0 \ \Rightarrow \ \text{for large} \ \eta: F'\to 0.\\ &\text{For large} \quad y: T\to T_1 \ \Rightarrow \ \text{for large} \ \eta: G\to 0.\end{aligned} \quad (25)$$

The rate of heat transfer to the wall is calculated as follows:

$$q_w=-k\left.\frac{\partial T}{\partial y}\right|_{y=0}=-k(T_w-T_1)\left.\frac{dG}{d\eta}\right|_{\eta=0}\frac{Gr_x^{0.25}}{x}. \quad (26)$$

Which gives us:

$$\frac{Nu_x}{Gr_x^{0.25}}=-G'|_{\eta=0} \quad (27)$$

The term Nu_x of Eq. (27) is the local Nusselt number.

4. Results and discussion

For the simulation by the similarity method of the laminar surface flow in free convection in a vertical flat plate, the numerical results are condensed in Table 1. Note here that we used the FORTRAN code to do our calculation.

The results indicated in this table are obtained for values of Pr equal to 0.7, 1, 3,10, and 30, and they represent the function $F(\eta)$ which varies with the similarity variable η, and its first and second derivative while the last column is reserved for the dimensionless temperature $\theta(\eta)$ in which, $F(\eta)$ here denotes the stream function , $F'(\eta)$ is the velocity profile and $F''(\eta)$ is the variation of shear stress.

Velocity profiles by varying Pr values are shown in Figure 3. Following the no-slip condition and close to the surface, it is evident that the fluid flow is stationary. By examining these curves, we can also see a great influence of the Prandtl number Pr on the flow velocity, the more Pr increases, the more the dimensionless velocity decreases. The velocity in a boundary layer close to the surface tends to a zero value and then it increases at the entrance of the plate passes through a maximum then gradually decreases to satisfy the condition at the exit, and this is due to the presence of strong viscous forces. The dimensionless velocity reaches maximum values and it has a tendency to move forward towards increasing values of η when Pr decreases.

Table 1. Numerical results obtained during the simulation.

η	F	$dF/d\eta$	$d^2F/d\eta^2$	$G = \theta$
		$Pr = 0.7$		
0.000000	0.000000	0.000000	0.958222	1.000000
0.030000	0.000427	0.028298	0.928382	0.989401
0.060000	0.001689	0.055706	0.898867	0.978802
0.120000	0.006614	0.107890	0.840832	0.957607
0.180000	0.014567	0.156633	0.784168	0.936416
0.300000	0.038744	0.244133	0.675141	0.894071
0.600000	0.138533	0.408852	0.429688	0.788871
0.900000	0.277311	0.506161	0.226292	0.685990
0.990000	0.323710	0.524137	0.173836	0.655887
1.005000	0.331591	0.526682	0.165481	0.650912
2.010000	0.870945	0.492243	-0.162656	0.359019
3.000000	1.267433	0.305737	-0.184709	0.173699
4.005000	1.491734	0.152027	-0.118203	0.075239
5.010000	1.595554	0.064257	-0.060586	0.029944
6.000000	1.635738	0.022342	-0.027574	0.010510
7.005000	1.647628	0.004109	-0.010770	0.002109
7.485000	1.648548	0.000084	-0.006277	0.000046
		$Pr = 1$		
0.000000	0.000000	0.000000	0.907472	1.000000
0.030000	0.000404	0.026776	0.877654	0.987974
0.060000	0.001598	0.052663	0.848201	0.975948
0.120000	0.006249	0.101814	0.790418	0.951898
0.180000	0.013747	0.147544	0.734166	0.927855
0.300000	0.036476	0.229114	0.626424	0.879824
0.600000	0.129639	0.379981	0.386588	0.760755
0.900000	0.257933	0.465553	0.191516	0.645177
0.990000	0.300540	0.480527	0.141927	0.611637
1.005000	0.307763	0.482597	0.134062	0.606110
2.010000	0.792700	0.433639	-0.161205	0.294568
3.000000	1.135384	0.258312	-0.167030	0.120571
4.005000	1.321415	0.123241	-0.100607	0.043239
5.010000	1.404281	0.050348	-0.048838	0.014265
6.000000	1.435495	0.017225	-0.021310	0.004229
7.005000	1.444688	0.003224	-0.008315	0.000735
7.485000	1.445416	0.000068	-0.005059	0.000015
		$Pr = 3$		
0.000000	0.000000	0.000000	0.750420	1.000000
0.030000	0.000333	0.022065	0.720680	0.982710
0.060000	0.001315	0.043246	0.691462	0.965421
0.120000	0.005120	0.083018	0.634610	0.930850
0.180000	0.011210	0.119442	0.579891	0.896303
0.300000	0.029466	0.182766	0.476959	0.827406
0.600000	0.102271	0.291671	0.258358	0.658609
0.900000	0.198743	0.343303	0.094841	0.501223
0.990000	0.229971	0.350059	0.056050	0.457521
1.005000	0.235228	0.350855	0.050023	0.450426
2.010000	0.566211	0.278395	-0.131940	0.120970
3.000000	0.778396	0.155236	-0.104720	0.021783
4.005000	0.890041	0.074910	-0.057546	0.002970
5.010000	0.941896	0.033106	-0.028648	0.000356
6.000000	0.963440	0.012810	-0.014035	0.000040
7.005000	0.970677	0.002801	-0.006758	0.000003
7.485000	0.971327	0.000064	-0.004764	0.000000

Table 1. Numerical results obtained during the simulation (continued).

η	F	$dF/d\eta$	$d^2F/d\eta^2$	$G = \theta$
		$Pr = 10$		
0.030000	0.000262	0.017319	0.562549	0.975221
0.060000	0.001030	0.033760	0.533667	0.950444
0.120000	0.003983	0.064100	0.478148	0.900915
0.180000	0.008658	0.091198	0.425636	0.851477
0.300000	0.022428	0.136395	0.329660	0.753323
0.600000	0.075088	0.205277	0.141710	0.519991
0.900000	0.141017	0.228272	0.021986	0.323021
0.990000	0.161615	0.229110	-0.002574	0.273921
1.005000	0.165052	0.229044	-0.006223	0.266229
2.010000	0.368975	0.166113	-0.078143	0.021041
3.000000	0.498698	0.100083	-0.054033	0.000639
4.005000	0.575785	0.056733	-0.033668	0.000010
5.010000	0.618238	0.029912	-0.020724	0.000000
6.000000	0.639145	0.013626	-0.012807	0.000000
7.005000	0.647309	0.003446	-0.007854	0.000000
7.485000	0.648125	0.000084	-0.006220	0.000000
		$Pr = 30$		
0.000000	0.000000	0.000000	0.467453	1.000000
0.030000	0.000206	0.013579	0.437958	0.966347
0.060000	0.000806	0.026288	0.409474	0.932700
0.120000	0.003087	0.049218	0.355543	0.865483
0.180000	0.006650	0.069034	0.305660	0.798556
0.300000	0.016915	0.100291	0.217954	0.666926
0.600000	0.054177	0.140501	0.065138	0.372451
0.900000	0.097886	0.147147	-0.010338	0.167114
0.990000	0.111070	0.145647	-0.022358	0.125544
1.005000	0.113252	0.145299	-0.024007	0.119452
2.010000	0.239589	0.104334	-0.040657	0.001182
3.000000	0.324821	0.069656	-0.029776	0.000001
4.005000	0.381309	0.044159	-0.021398	-0.000001
5.010000	0.415992	0.025880	-0.015311	-0.000001
6.000000	0.434872	0.012973	-0.011000	-0.000001
7.005000	0.442927	0.003581	-0.007867	-0.000001
7.485000	0.443786	0.000091	-0.006705	-0.000001

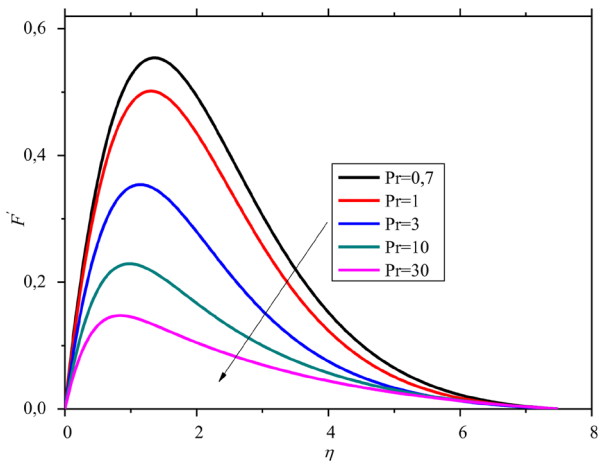

Figure 3. Evolution of the dimensionless velocity during variable η according to Pr.

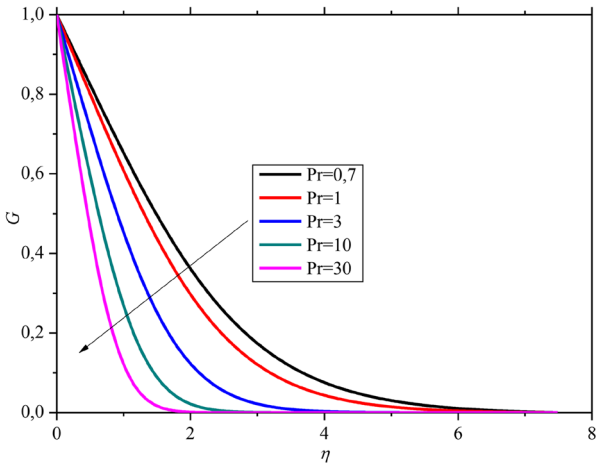

Figure 4. Variation of dimensionless temperature as a function of η.

Figure 4 depicts the temperature profiles along η for values of Prandtl equal to, 0.7, 1, 3, 10, and 30. We can also see a great influence of Pr on the heat transfer rate, the more Pr increases, the more the thermal boundary layer decreases.

The Prandtl number quantifies the relative rapidity of a medium to transfer energy by convection or conduction; the higher it is, the more the movements of matter explain the temperature profiles of the medium. An increasing value of Pr indicates increasing viscous effects.

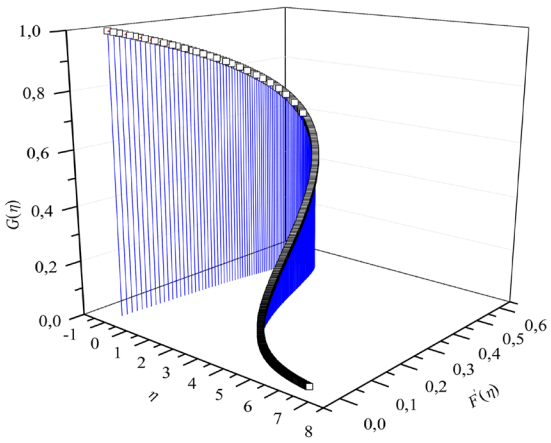

Figure 5. 3D Evolution of temperature.

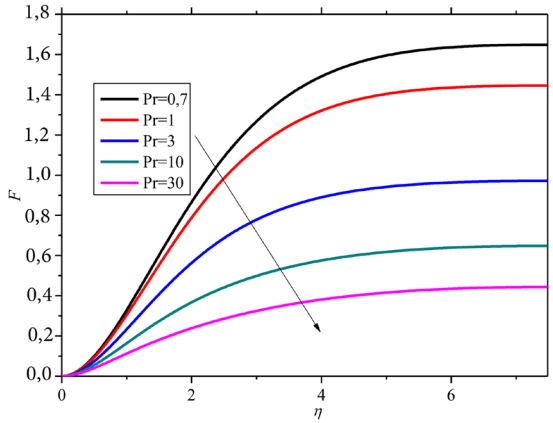

Figure 6. Contour of F with η for variable Pr.

We have depicted in Figure 5 a three-dimensional 3D model of the dimensionless temperature as a function of η and $F'(\eta)$ on the two axes. We can notice that the temperature of the fluid tends to become maximum then, it gradually decreases to zero value on the plate so as to ensure the boundary condition.

The bundle of curves of the function $F(\eta)$ shown in Figure 6 for the different values of Pr indicate a strong influence on the behavior of the flow within the boundary layer. We notice that for low values of Pr, the function $F(\eta)$ behaves gradually by developing a boundary layer at the entrance of the plate and stabilizing at the end towards a constant value.

The Prandtl number physically characterizes the relative thickness of the thermal and kinetic boundary layers. When the thermal diffusivity decreases and the viscous force increases, this gives rise to Pr which causes the coefficient of friction to decrease.

We have represented in Figure 7 the profiles of function F and its derivatives F' and F'' as a function of η but only at the value of $Pr = 0.7$. We can distinguish that the evolution of the function F' has the same behavior of the speed while that of the function F'' also follows the behavior of the temperature.

We studied the effect of the Prandtl number involved in the parietal heat transfer. For this, we plotted in Figure 8 the profile of $\frac{d_2F}{d\eta_2}$ with η by varying Pr. Since the velocity vector increases steadily over time in moving away from the plate to reach its maximum altitude at the level of the boundary layer then decreases from the hot wall and tends towards

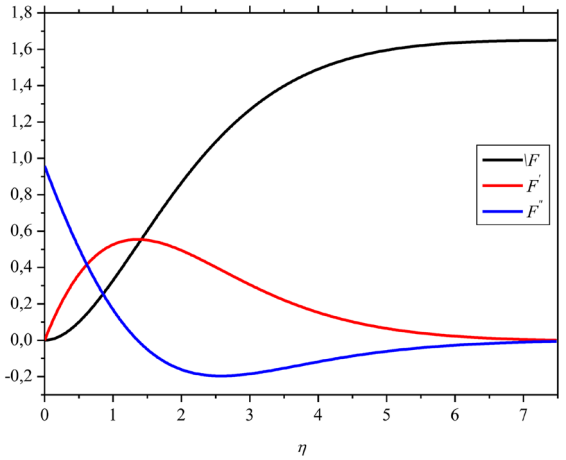

Figure 7. Behavior of F, F', and F'' as a function of η.

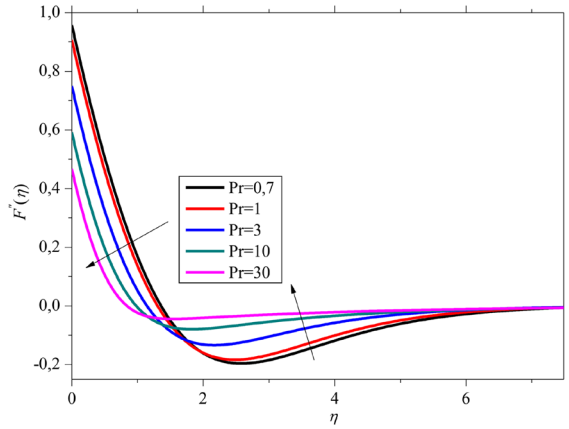

Figure 8. Variation of the profile of the function $d^2F/d\eta^2$ for different values of Pr

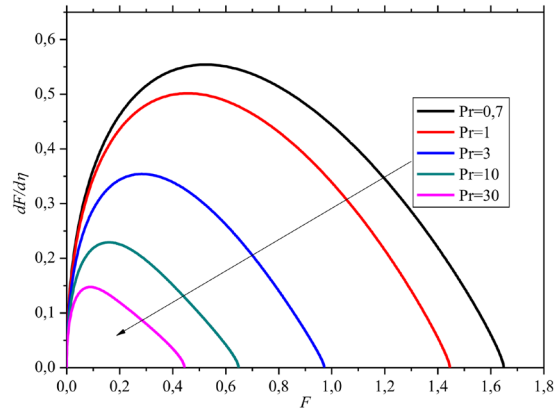

Figure 9. Variation of the velocity profile $dF/d\eta$ with respect to F for various values of Pr.

zero. This decrease in the maximum speed can directly come from the decrease in temperature on the heated vertical wall which leads to a reduction in the buoyancy forces. A robust shear stress gradient can be compromised through this mechanism. The graph shows that the temperature of the fluid flow is highest just near the plate and it decreases exponentially towards a value close to zero once the heat transfer is complete.

Figure 9 represents the evolution of velocity profiles $dF/d\eta$ following the variation of $F(\eta)$ for the values of $Pr = 0{,}7{,}1{,}3{,}10$ and 30. It is evident that the shape of the velocity field disposed is well structured and elliptical and that the parameter of the Prandtl number has a lag effect on

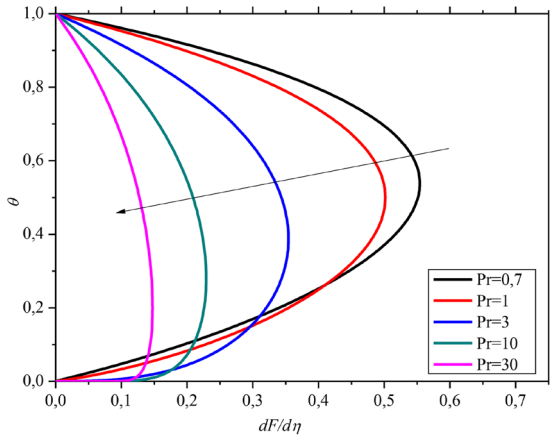

Figure 10. Variation of temperature as a function of velocity for different values of the Prandtl number.

the fluid velocity. We observe that the speed $F'(\eta)$ increases with the decrease of Pr and that its value is greater near $Pr = 0.7$. This is due to the increase in the dynamic viscosity of the fluid.

In Figure 10, we have presented in the boundary layer, the variation of the dimensionless temperature profile for different values of Pr and as a function of velocity. It can be seen that the increase in Pr leads to a decrease in both the velocity and temperature parameters and also in the thickness of the thermal boundary layer which rises in the direction of the flow.

Table 2 below represents the values of A which were evaluated by varying the Prandtl number Pr.

The values of G were estimated approximately from which LeFevre [30] was able to evaluate this shape taken from the numerical approximation:

$$\frac{Nu_x}{Gr_x^{0.25}} = -G'|_{\eta=0} = \left[\frac{0.316\ Pr^{5/4}}{2.44 + 4.88\ Pr^{1/2} + 4.95\ Pr}\right]^{1/4} \quad (28)$$

The average rate of heat transfer along plate L is calculated as follows:

$$\overline{q_w} = \frac{1}{L}\int_0^L q_w dx. \quad (29)$$

By using the Eq. (26), we get:

$$\overline{q_w} = \frac{1}{L}\int_0^L \left[-k(T_w - T_1)G'|_{\eta=0}\frac{Gr_x^{0.25}}{x}dx\right],$$

$$\frac{\overline{q_w}L}{(T_w - T_1)k} = G'|_{\eta=0}\frac{4}{3}Gr_L^{0.25}.$$

With Gr_L is the estimated Grashof number along a flat plate of length L.

We can then express the average Nusselt number N_{u_L} on the entire plate:

$$\frac{Nu_L}{Gr_L^{0.25}} = \frac{4}{3}G'|_{\eta=0}. \quad (30)$$

5. Comparison and validation of results

To illustrate the accuracy of the solution of our numerical model obtained by the similarity method, and to do this, we conducted bibliographic research in a methodical and well-founded way to be effective and to know the investigations

Table 2. Values of A calculated as a function of Pr.

Pr	$A = -G'\|_{\eta=0}$	$-G'\|_{\eta=0}/Pr^{0.25}$
0.01	0.0570	0.1802
0.03	0.0962	0.2312
0.09	0.1549	0.28287
0.72	0.3568	0.3873
1	0.4010	0.4010
2	0.5066	0.4260
5	0.6746	0.4511
10	0.8259	0.4644
100	1.549	0.4898
1000	2.807	0.4992

Table.3. Comparison of literature results with those of the numerical model.

η	Present work $\theta(\eta)$	Similarity analysis $\theta(\eta)$ [27]	Similarity analysis $\theta(\eta)$ [28]
0	1.0000	1.0000	1.0000
1	0.6509	0.6435	0.6526
2	0.3590	0.3745	0.3615
3	0.1737	0.1992	0.1741
4	0.0752	0.0978	0.0767
5	0.0299	0.0448	0.0284
6	0.0105	0.0193	0.0102
7	0.0021	0.0078	0.0015

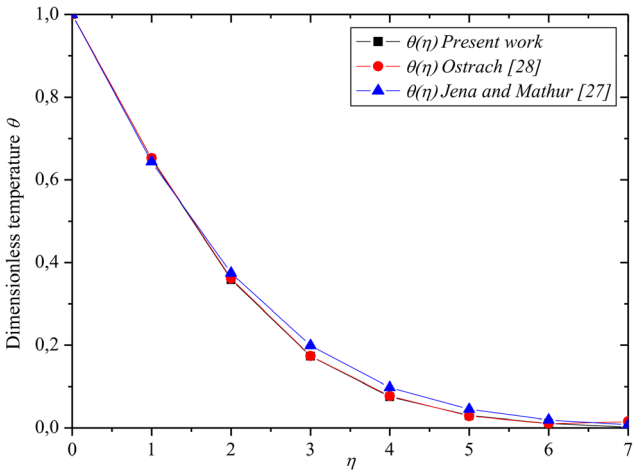

Figure 11. Comparison with reference results from the literature.

that were carried out and related to the subject of this work. We were able to discover there the work of numerical simulations which were made by Jena and Mathur [27] and Ostraque [28] to carry out more the comparison. We have thus summarized in Table 3 the numerical simulation results of our study with those of previous research published by these authors.

We found that our results are almost similar to those presented by the other authors with respect to dimensionless temperature, which means that the comparison gives better good certainty to our model and shows good agreement.

We have plotted graphically in Figure 11, the three above-mentioned digital models from which we have found that the temperature profiles for the three speeds are practically coincident. It turned out that the model developed by Ostrach [28] represents a remarkable convergence

excellence when compared to that of our work. Finally, we conclude that the results of the simulation performed in this work show a very good agreement with those found in the literature.

Conclusion

The predictive analysis of heat transfer of a laminar flow of natural convection on a vertical flat plate was carried out here from similarity variables made numerically.

In the studied configuration, we needed some assumptions to reduce the solution of the Navier-Stokes equations describing the laminar flow of the fluid into a simple model, placed in a stable two-dimensional state. For this, the properties of the fluid were considered constant except the variation of the density is mainly dependent on the temperature while neglecting the effect of viscous dissipation.

After having introduced the assumptions which make it possible to reduce the study of a complex flow to the study of a simple problem, and to apply the boundary conditions, we resorted to the adimensionalization of the variables associated with the method of similarity to bring the governing partial differential equations back to the ordinary equations on which we have integrated them by the Runge-Kutta method of order 04.

We have developed a program in FORTRAN allowing us to solve these equations whose initial data introduced there, were in terms of Prandtl number, and varied each time in the compilation.

The emerging results of this study are summarized as follows:

- The increase in the Prandtl number leads to a decrease in the thickness of the thermal boundary layer;
- The greater the temperature gradient, the higher the Prandtl number and this is evident from the physical significance of the Pr number which compares motion diffusivity and thermal diffusivity;
- When the value of the viscosity of the fluid increases, the number of Prandtl Pr also increases;
- The viscous forces are proportional to the speed gradient, and when these increase, the maximum speed decreases for high Pr;
- The position of the maximum value of the dimensionless velocity has a tendency to move towards increasing η when the value of Pr decreases;
- The dimensionless maximum temperature coordinate has a tendency to move towards high η when Pr increases;
- The thickness of the velocity boundary layer reaches high values when Pr decreases;
- The numerical results of the simulation obtained by the computer code have been validated and reveal that they are in good agreement with those already published in the literature.

Although the main results presented in this work form a coherent whole, other topics for further research should be carried out in order to elucidate, especially the verification of the results obtained experimentally.

Nomenclature

C_p	Specific heat at constant pressure, [J kg^{-1} K^{-1}]
F	Dimensionless stream function
G	Dimensionless temperature
Gr	Grashof number
Gr_L	Grashof number based on the plate length, L
Gr_x	Grashof number based on x
g	Gravitational acceleration, [ms^{-2}]
$\vec{g}$	Gravity vector, [ms^{-2}]
k	Thermal conductivity, [Wm^{-1}K^{-1}]
L	Length, [m]
Nu	Nusselt number
Nu_x	Local Nusselt number
p	Pressure [kg m s^{-2}]
p'	Piezometric pressure [kg m s^{-2}]
Pr	Prandtl number
q	Heat transfer rate per unit area, [Wm^{-2}]
q_w	Local heat transfer rate per unit area at wall, [Wm^{-2}]
$\overline{q_w}$	Mean heat transfer rate, [Wm^{-2}]
q'''	Internal heat generation, [Wm^{-3}]
t	Time, [s]
T	Temperature, [K]
T_1	Fluid temperature, [K]
T_w	Wall temperature, [K]
U	Dimensionless velocity
u	Velocity component, [ms^{-1}]
u_r	Fluid velocity, [ms^{-1}]
V	Dimensionless velocity
$\vec{V}$	Velocity vector
v	Velocity component, [ms^{-1}]
w	Velocity component, [ms^{-1}]
x	Distance, [m]
x	Coordinate direction, [m]
y	Coordinate direction, [m]
z	Coordinate direction, [m]

Greek letters

β	Thermal expansion, [K^{-1}]
δ	Velocity boundary layer thickness, [m]
δ_{th}	Thermal boundary layer thickness, [m]
η	Similarity variable, [m]
θ	Dimensionless temperature
μ	Dynamic viscosity, [kgm^{-1}s^{-1}]
υ	Kinematic viscosity, [m^{2}s^{-1}]
ρ	Density, [kgm^{-3}]
ρ_0	Initial density, [kgm^{-3}]
φ	Angular coordinate, [°]
Φ	Dissipation function
$\frac{D}{Dt}$	Material derivative operator
∇	Nabla operator
∇^2	Laplace operator
$\boldsymbol{\partial}$	Partial derivative operator

Funding

This research did not receive any specific grant from funding agencies in the public, commercial, or not-for-profit sectors.

Conflicts of interest

The authors declare that they have no known competing financial interests or personal relationships that could have

appeared to influence the work reported in this paper.

Authors contribution statement

Frist author

Ali Belhocine: Conceptualization; Investigation; Methodology; Validation; original draft; Writing - review & editing.

Second author

Nadica Stojanovic: Data curation; Formal analysis; Software; Visualization

Third author

Oday Ibraheem Abdullah: Project administration; Resources; Supervision; Roles/Writing

References

1. Nouri-Borujerdi, A. and Sepahi, F. "Effect of several heated interior bodies on turbulent natural convection in enclosures", *Scientia Iranica,* **26**(3), pp. 1335-1349 (2019). https://doi.org/10.24200/sci.2018.20588

2. Bhuvaneswari, M., Eswaramoorthi, S., Sivasankaran, S., et al. "Effects of viscous dissipation and convective heating on convection flow of a second-grade liquid over a stretching surface: An analytical and numerical study", *Scientia Iranica,* **26**(3), pp. 1350-1357 (2019). https://doi.org/10.24200/sci.2018.20414

3. Sepahi-Younsi, J., Soltani, M.R., Abedi, M., et al. "Experimental investigation into the effects of Mach number and boundary-layer bleed on flow stability of a supersonic air intake", *Scientia Iranica,* **27**(3), pp. 1197-1205 (2020). https://doi.org/10.24200/sci.2019.21683

4. Saeidinezhad, A., Dehghan, A.A., and Dehghan Manshadi, M. "Boundary layer and surface pressure distribution behavior over a submarine nose model with two different nose shapes", *Scientia Iranica,* **27**(3), pp. 1277-1289. (2020). https://doi.org/10.24200/sci.2019.50454.1703

5. Golkar, S.H., Khayat, M., and Zareh, M. "Experimental study of heat transfer characteristics of nanofluid nucleate and film boiling on horizontal flat plate", *Scientia Iranica,* **28**(6), pp. 3216-3231 (2021). https://doi.org/10.24200/sci.2021.56967.4997

6. Shakiba, A. and Rahimi, A.B. "Role of movement of walls with time-dependent velocity on flow and mixed convection in vertical cylindrical annulus with suction/injection", *Scientia Iranica,* **28**(3), pp. 1306-1317 (2021). https://doi.org/10.24200/sci.2020.54784.3917

7. Lakshmi Devi, G., Niranjan, H., and Sivasankaran, S. "Effects of chemical reactions, radiation, and activation energy on MHD buoyancy induced nanofluid flow past a vertical surface", *Scientia Iranica,* **29**(1), pp. 90-100 (2022). https://doi.org/10.24200/sci.2021.56835.4934

8. Mokaddes Ali, M., Rushd, S., Akhter, R., et al. "Magneto-hydrodynamic mixed convective heat transfer in a nanofluid filled wavy conduit with rotating cylinders", *Scientia Iranica,* **29**(2), pp. 486-501 (2022). https://doi.org/10.24200/sci.2021.56422.4717

9. Ibitoye, S.E., Adegun, I.K., Olayemi, O.A., et al. "Experimental and numerical investigation of flow behaviors of some selected food supplements in modeled intestine", *Scientia Iranica,* **30**(1), pp. 39-51 (2023). https://doi.org/10.24200/sci.2022.60130.6613

10. Khader, M.M., Inc, M., and Akgul, A. "Numerical appraisal of the unsteady Casson fluid flow through Finite Element Method (FEM)", *Scientia Iranica,* **30**(2), pp. 454-463 (2023). https://doi.org/10.24200/sci.2022.60176.6644

11. Alomar, O.R., Basher, N.M, and Yousif, A.A. "Natural convection heat transfer from a bank of orthogonal heated plates embedded in a porous medium using LTNE model: A comparison between in-line and staggered arrangements", *International Journal of Thermal Sciences,* **160**, 106692 (2021). https://doi.org/10.1016/j.ijthermalsci.2020.106692

12. Shah, N.A., Awan, A.U., Khan, R., et al. "Free convection Hartmann flow of a viscous fluid with damped thermal transport through cylindrical tube", *Chinese Journal of Physics*, **80**, pp. 19-33 (2022). https://doi.org/10.1016/j.cjph.2021.09.019

13. Awan, A.U., Ali, Q., Riaz, S., et al. "A thermal optimization through an innovative mechanism of free convection flow of Jeffrey fluid using non-local kernel", *Case Studies in Thermal Engineering*, **24**, 100851 (2021). https://doi.org/10.1016/j.csite.2021.100851

14. Awan, A.U., Riaz, S., Sattar, S., et al. "Fractional modeling and synchronization of ferrofluid on free convection flow with magnetolysis", *The European Physical Journal Plus*, **135**, 841 (2020). https://doi.org/10.1140/epjp/s13360-020-00852-4

15. Qasim, A., Riaz, S., and Awan, A.U. "Free convection MHD flow of viscous fluid by means of damped shear and thermal flux in a vertical circular tube", *Physica Scripta*, **95**(9), 095212 (2020). http://dx.doi.org/10.1088/1402-4896/abab39

16. Awan, A.U., Shah, N.A., Ahmed, N., et al. "Analysis of free convection flow of viscous fluid with damped thermal and mass fluxes", *Chinese Journal of Physics,* **60**, pp. 98–106 (2019). https://doi.org/10.1016/j.cjph.2019.05.006

17. Kim, K.M., Lim, S.T., Kim, S.H., et al. "Transition phenomena of natural convection of the air in an asymmetrically heated vertical channel with a damper", *International Journal of Heat and Mass Transfer,* **183**, Part C, 122196 (2022). https://doi.org/10.1016/j.ijheatmasstransfer.2021.122196

18. Kandaswamy, P., Abdul Hakeem, A.K., Saravanan, S. "Internal natural convection driven by an orthogonal pair of differentially heated plates", *Computers and Fluids,* **111**, pp. 179-186 (2015). https://doi.org/10.1016/j.compfluid.2015.01.015

19. Ismaeel, A.M., Mansour, M.A., Ibrahim, F.S., et al. "Numerical simulation for nanofluid extravasation from a vertical segment of a cylindrical vessel into the surrounding tissue at the microscale", *Applied Mathematics and Computation,* **417**, 126758 (2022). https://doi.org/10.1016/j.amc.2021.126758

20. Hady, F., Ibrahim, F., El-Hawary, H., et al. "Effect of suction/injection on natural convective boundary-layer flow of A nanofluid past a vertical porous plate through a porous medium", *International Journal of Heat and Fluid Flow,* **3**(1), pp. 53-63(2012). http://dx.doi.org/10.20454/jmmnm.2012.169

21. Talluru, K.M., Pan, H.F., Patterson, J.C., et al. "Convection velocity of temperature fluctuations in a natural convection boundary layer", *International Journal of Heat and Fluid Flow,* **84**, 108590 (2020). https://doi.org/10.1016/j.ijheatfluidflow.2020.108590

22. Belhocine, A. and Wan Omar, W.Z. "An analytical method for solving exact solutions of the convective heat transfer in fully developed laminar flow through a circular tube", *Heat Transfer Asian Research,* **46**(8), pp. 1342-1353 (2017). https://doi.org/10.1002/htj.21277

23. Belhocine, A. and Wan Omar, W.Z. "Numerical study of heat convective mass transfer in a fully developed laminar flow with constant wall temperature", *Case Studies in Thermal Engineering,* **6**, pp. 43-60 (2015). https://doi.org/10.1016/j.csite.2015.08.003

24. Belhocine, A. and Abdullah, O.I. "Numerical simulation of thermally developing turbulent flow through a cylindrical tube", *The International Journal of Advanced Manufacturing Technology,* **102**(5-8), pp. 2001–2012 (2019). https://doi.org/10.1007/s00170-019-03315-y

25. Belhocine, A. and Wan Omar, W.Z. "Analytical solution and numerical simulation of the generalized Levèque equation to predict the thermal boundary layer", *Mathematics and Computers in Simulation,* **180**, pp. 43–60 (2021). https://doi.org/10.1016/j.matcom.2020.08.007

26. Belhocine, A., Stojanovic, N., and Abdullah, O.I. "Numerical simulation of laminar boundary layer flow over a horizontal flat plate in external incompressible viscous fluid", *European Journal of Computational Mechanics,* **30**(4-6), pp. 337-386 (2021). http://dx.doi.org/10.13052/ejcm2642-2085.30463

27. Jena, S.K. and Mathur, M.N. "Similarity solutions for laminar free convection flow of a thermomicropolar fluid past a non-isothermal vertical flat plate", *International Journal of Engineering Science,* **19**(2), pp. 1431-1439 (1981). https://doi.org/10.1016/0020-7225(81)90040-9

28. Ostrach, S. "An analysis of laminar free convection flow and heat transfer about a flat plate parallel to the direction of the generating body force", *National Advisory Committee for Aeronautics*, Report 1111, (1953).

29. Yıldız, S. "Investigation of natural convection heat transfer at constant heat flux along a vertical and inclined plate", *Journal of Thermal Engineering*, **4**(6), pp. 2432-2444 (2018). https://doi.org/10.18186/thermal.465654

30. LeFevre, E.J. "Laminar free convection from a vertical plane surface". *International Journal of Heat and Mass Transfer,* Brussels, **4**, p. 168 (1956). http://dx.doi.org/10.1016/0017-9310(84)90008-5

Biographies

Ali Belhocine received his Magister degree in Mechanical Engineering in 2006 from Mascara University, Mascara, Algeria. After then, he has obtained his PhD degrees in Mechanical Engineering in 2012 at the University of Science and the Technology of Oran, USTO Oran, Algeria. His research interests include Automotive Braking Systems, Finite Element Method (FEM), ANSYS simulation, CFD Analysis, Heat Transfer, Thermal-Structural Analysis, Tribology and Contact Mechanic.

Nadica Stojanovic, Assistant Professor, doctorate degree obtained at the University of Kragujevac, Faculty of Engineering. Scientific fields – Motor vehicles and motors. Her research areas cover FE analysis, thermal-mechanical analysis, aerodynamics, ergonomics, and environmental science. Workplace – assistant professorat the University of Kragujevac, Faculty of engineering. She participates in the project "Research on vehicle safety as part of the cybernetic system: driver - vehicle - environment" of the Ministry of Education, Science and Technological Development of the Republic of Serbia.

Oday Ibraheem Abdullah, is a Univ.-Professor at University of Baghdad (Energy Engineering Department, College of Engineering) since 2002. Also, He is Research Associate at Hamburg University of Technology since 2015 and Gulf University since 2023. He received his PhD degree in mechanical engineering from Hamburg University of Technology in 2015. His research areas cover the tribology, stress analysis, vibration analysis, renewable energy and thermal analysis.